

Bunch Compressor for the TESLA Linear Collider

W. Decking, G. Hoffstaetter, T. Limberg
DESY, Notkestraße 85, 22603 Hamburg, Germany

September 2000

Abstract

We discuss different bunch compression systems for the TESLA collider. The best alternative is a wiggler type compressor, where we list the important parameters. Systems which allow a manipulation of higher order effects have been analyzed in detail and their limitations are derived.

1 Introduction

In linear colliders, the beams have to be reduced in emittance in damping rings. The lower limit on DR bunch length because of wake-field induced instabilities or power considerations for the RF system is a few millimeters, too long for optimal operation of the collider. A bunch compression system has to shorten the bunch before injection into the main linac.

Bunch compression for relativistic particles can only be achieved by inducing a correlation between longitudinal position and energy offset with an RF system and making use of the path length differences in a following dispersive beam line section (e.g., a magnet chicane) to bring head and tail of the bunch closer together. To overcome the initial energy spread $\sigma_{\delta i}$, the RF induced energy correlation must increase the energy spread after compression to:

$$\sigma_{\delta f} = \sigma_{\delta i} \cdot \frac{\sigma_{z i}}{\sigma_{z f}} \quad (1)$$

with $\sigma_{z i}$ the bunch length out of the damping ring and $\sigma_{z f}$ the final bunch length. From the induced energy spread then follows the necessary 'longitudinal dispersion' $R_{56} = \Delta z / \delta$:

$$R_{56 \text{ needed}} = \frac{\sqrt{\sigma_{z i}^2 - \sigma_{z f}^2}}{\sigma_{\delta f}} \quad (2)$$

The basic parameters for the TESLA bunch compressor are given in table 1.

The required big compression ratio ($\sigma_{z i} / \sigma_{z f} \approx 18$) and the non-negligible incoming uncorrelated momentum spread necessitate a large momentum spread of nearly 3%

Table 1: Target parameters for the TESLA bunch compressor

horizontal input emittance ε_x	8×10^{-6} m
vertical input emittance ε_y	0.02×10^{-6} m
input bunch length σ_{zi}	6×10^{-3} m
DR ejection momentum spread $\sigma_{\delta i}$	0.13 %
DR ejection energy E_0	5 GeV
final bunch length σ_{zf}	0.3×10^{-3} m
final momentum spread $\sigma_{\delta f}$	2.7×10^{-2} m
R_{56} of compressor chicane	0.23 m
Total RF voltage @ zero crossing needed	725 MV

RMS in the dispersive section. Higher order terms like the second order momentum compaction have to be taken into account. Chapter 2 describes a possible cancelation of higher order momentum compaction and nonlinearities in the RF wave form.

The beam line section supplying the necessary R_{56} must not increase transverse beam emittance due to incoherent or coherent synchrotron radiation. Both set constraints on the usable strength of bending magnets. So even if the compression is done in one stage, the total length of the compressor is of the order of a hundred meters.

A simple solution is a wiggler chicane as presented in chapter 3. Its main disadvantage is that its second order longitudinal dispersion R_{566} curves the longitudinal phase space so much that the required bunch length cannot be achieved if not compensated for by the upstream RF system. This necessary compensation scheme causes a deceleration of about 0.4 GeV.

In chapter 4 we present efforts to avoid this deceleration by using a compressor type where the R_{566} can be adjusted. In the so-called FODO type compressor, the dispersion is shaped with quadrupole magnets and the R_{566} can be adjusted by sextupole magnets. Up to now we could not find a sextupole scheme with a tolerable transverse emittance growth. Attachment 1 gives basic ideas and concepts to find optical schemes where the R_{566} is zero and the optics distortion by the necessary sextupole magnets do cancel and why it is hard to find them.

Since the preservation of emittance is such a central question for the TESLA collider the solution of choice at this moment is the simple wiggler chicane.

2 A Second Order Compensation Scheme

In the case of non-zero second order longitudinal dispersion R_{566} the resulting longitudinal phase space distortion can be canceled by proper choice of the R_{56} and the accelerating voltage phase and amplitude. Consider a particle passing through an RF-system with phase ϕ and accelerating voltage V . The final relative energy deviation is

in 2nd order:

$$\begin{aligned}\delta_f &= A\delta_i + Bz_i + Cz_i^2 \\ &= \frac{E_i}{E_f}\delta_i - \frac{2\pi V \sin \phi}{\lambda E_f}z_i - \frac{2\pi^2 V \cos \phi}{\lambda^2 E_f}z_i^2\end{aligned}\quad (3)$$

with E_i the initial energy, E_f the final energy, δ_i the initial relative energy deviation, and z_i the initial longitudinal particle position. The final longitudinal coordinate z_f of the particle after passage through a downstream dispersive beam line section is in 2nd order:

$$z_f = z_i + R_{56}\delta_f + R_{566}\delta_f^2. \quad (4)$$

Combining these two equations yields:

$$\begin{aligned}z_f &= AR_{56}\delta_i + (1 + BR_{56})z_i + (R_{56}C + R_{566}B^2)z_i^2 \\ &\quad + A^2R_{566}\delta_i^2 + 2ABR_{566}\delta_i z_i \\ &\quad + 2BCR_{566}z_i^3 + 2ACR_{566}\delta_i z_i^2 + C^2R_{566}z_i^4\end{aligned}\quad (5)$$

Figure 1 shows the necessary accelerating phase, gradient, and R_{56} to cancel the terms in z to 2nd order for various ratios $r = R_{566}/R_{56}$.

The necessary accelerating voltage is smallest for $r = 0$. For positive r the RF-phase has to be tuned to accelerate the bunch, while for negative ratios r the bunch is decelerated.

For large second order dispersions other higher order terms cannot be neglected. For ratios r below or above ± 1.5 the second order effects will distort the final longitudinal phase space and lead to a larger final bunch length.

3 Wiggler compressor

The wiggler compressor consists of bending magnet chicanes (wiggler) embedded in a FODO structure. No additional optical elements are included between the bending magnets of each wiggler section. In this case the dispersion is zero up to any order at the end of each wiggler section. The drawback is that the ratio r cannot be influenced. For any wiggler or chicane based bunch compressor r is ≈ -1.5 . The second order effects of this non-zero R_{566} can be compensated with the bunch compressor RF tuned to a decelerating phase as described above. The required accelerating voltage before the wiggler is 890 MV at a phase $\phi = 113$ deg. The final energy is 4.6 GeV. The total length of the bunch compressor (including some matching and 4 accelerating modules with an average gradient of 25 MV/m) amounts then to ≈ 165 m.

The optics of the wiggler compressor and the geometrical layout is shown in figure 2. The maximum deviation from the middle axis is 0.3 m, which should fit easily in the main linac tunnel. Tracking of particles which are randomly distributed in the six-dimensional phase space with a maximum amplitude of 3σ using the code MAD[5] shows no significant emittance growth. Figure 3 shows the longitudinal phase space, while figures 4 and 5 show the horizontal respectively vertical phase space before and after the bunch compressor.

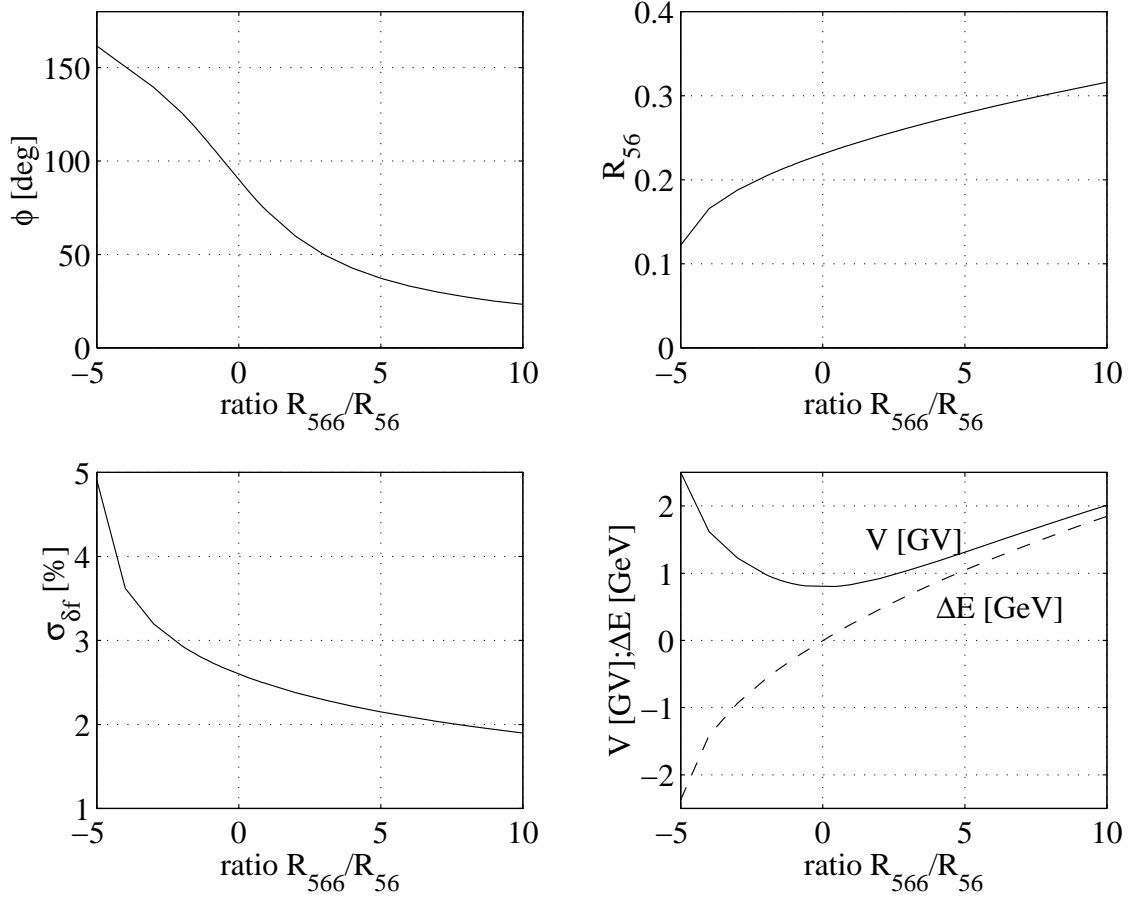


Figure 1: Accelerating phase, R_{56} , final energy spread, and effective accelerating voltage (in descending order) for a bunch length of $300 \mu\text{m}$ and various ratios r .

Table 2: Parameters of the Wiggler Bunch Compressor

R_{56}	0.215 m
$\sigma_{\delta f}$	2.8 %
V_{RF}	890 V
ϕ_{RF}	113 deg
total length	86.4 m
$\Delta\varepsilon_{x;sync.rad.}$	2.2×10^{-8} m
bend angle	3.23 deg, 6.46 deg
bend field	0.44 T
number of bends	12, 6
quadrupole length	0.2 m
quadrupole gradient	6.5 T/m
number of quadrupoles	7

The final check for the wiggler performance is a calculation of emittance growth due to Coherent Synchrotron Radiation effects. The code TraFiC4 models the incoming bunch as a line of Gaussian 3-d sub-bunches which are tracked through the dispersive beam line section, generating the electro magnetic fields. The action of the field on the generating sub-bunches leads to correlated offsets of their centers. In addition, an ensemble of a few hundred test particles which are longitudinally positioned close to the bunch-center are tracked through the fields to probe for uncorrelated transverse emittance growth. From both ensembles, the projected emittance is calculated (see figure 6). The correlated emittance oscillates because linear dispersive offsets are subtracted but not quadratic ones. At the compressor exit, the correlated emittance (normalized) is about $2.5 \cdot 10^{-7}$ m, the uncorrelated emittance is preserved and the projected emittance grows by less than 5%. The parameters for the wiggler type compressor are presented in the table 2.

4 FODO compressor

Most efficient use of the RF system requires a compressor with a positive r . As an example serves a so called FODO compressor. It consists of a FODO channel with bending magnets forming a chicane. The optics and the layout for this design is shown in figure 7. Note that that the compact design (40 m length) requires a transverse deviation of about 2.5 m at the midpoint; more reasonable values of less than a meter would result in overall length comparable to the wiggler chicane.

The FODO compressor has a positive ratio $r \approx 10$. This allows in principle to operate the bunch compressor RF with an accelerating phase. Unfortunately, according to chapter 2 higher order terms distort the 2nd order compensation if r assumes values above 3/2. However, sextupoles can be employed to tune r . At a value of 3/2, compression could be done with an accelerating voltage of 900 MV and an energy gain

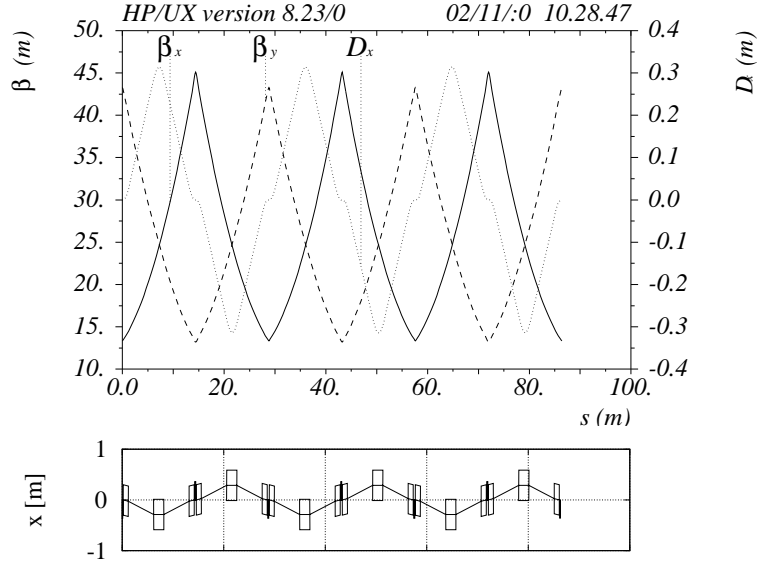


Figure 2: Optical functions of the wiggler bunch compressor.

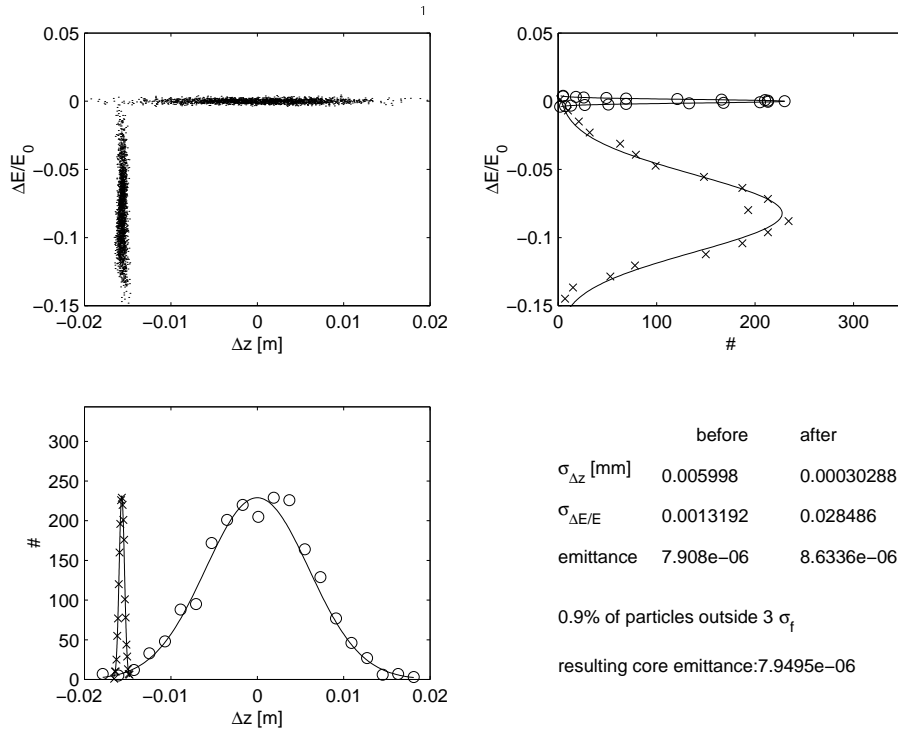


Figure 3: Longitudinal phase space before (circles) and after (crosses) the bunch compressor.

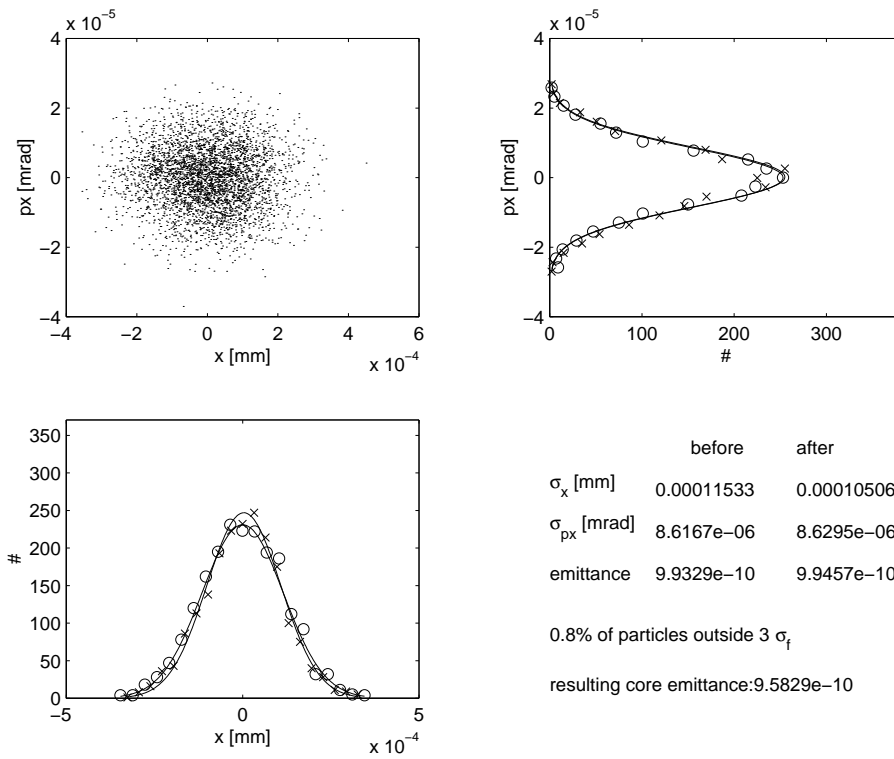


Figure 4: Horizontal phase space before (circles) and after (crosses) the bunch compressor.

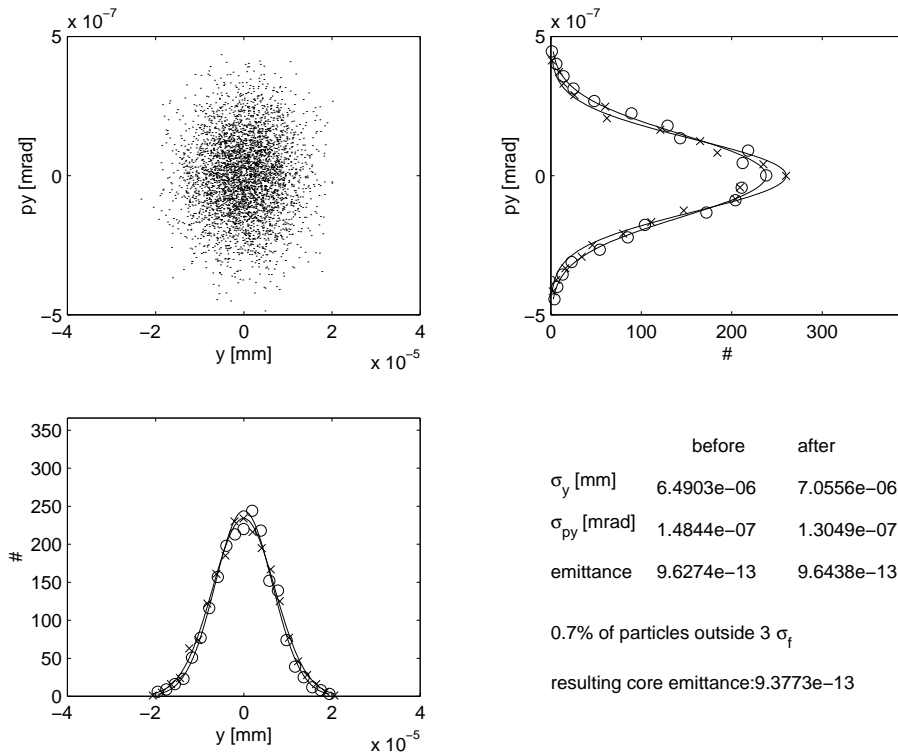


Figure 5: Vertical phase space before (circles) and after (crosses) the bunch compressor.

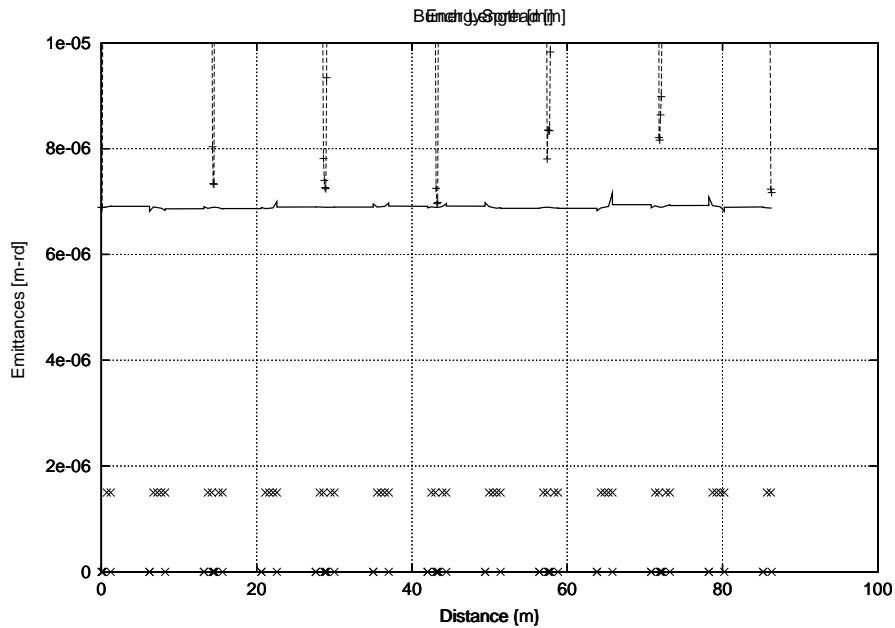


Figure 6: TraFiC4-calculation of emittance growth due to Coherent Synchrotron Radiation effects. Drawn line: slice emittance; dotted line: projected emittance. The bending magnets are indicated by the 'x' dots.

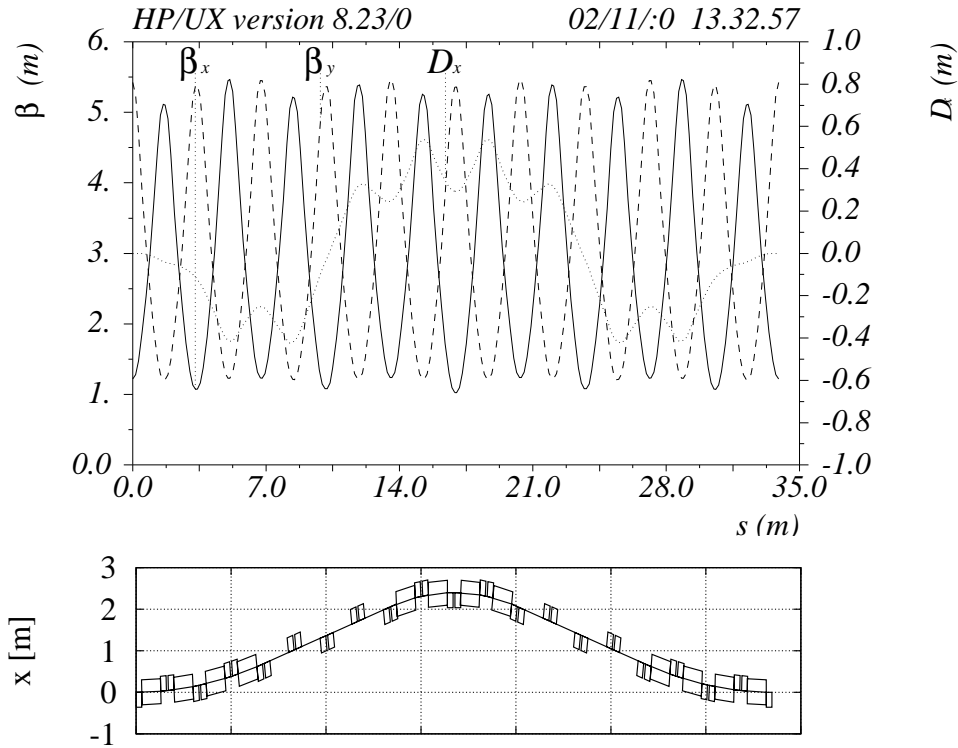


Figure 7: Layout of the FODO bunch compressor.

of 400 MeV, which corresponds to two RF modules.

In this case the nonlinear terms which are introduced by the sextupoles distort the trajectories of off-energy particles and cause emittance growth. To avoid this problem an achromat in very high order for $\Delta p/p_0 = \pm 10\%$ is needed.

5 Correction of R_{566}

In case of the described wiggler compressor, $R_{566}/R_{56} \approx -1.5$ is negative and therefore the beam would have to be decelerate by about 400 MeV in the compressor. In the FODO compressor this ratio is positive but very large and therefore nonlinear particle motion leads to a blowup of the longitudinal emittance. We therefore tried to minimize R_{566} for the required $|R_{56}| \approx 0.24$. For this optimization some basic formulae will be derived.

The reference particle travels on the design curve and has the coordinates $(x, y) = 0$. In order to find R_{56} and R_{566} , one needs to know the trajectory $(x(\delta), y(\delta))$ of a particle that starts on the design curve with a relative momentum deviation δ from the design momentum p_0 . Since the path length of a trajectory $\vec{r}(l)$ is given by

$$|d\vec{r}| = \sqrt{(1 + x/\rho_0)^2 + x'^2 + y'^2} dl, \quad (6)$$

the difference in traveled path with respect to the reference particle at position L along

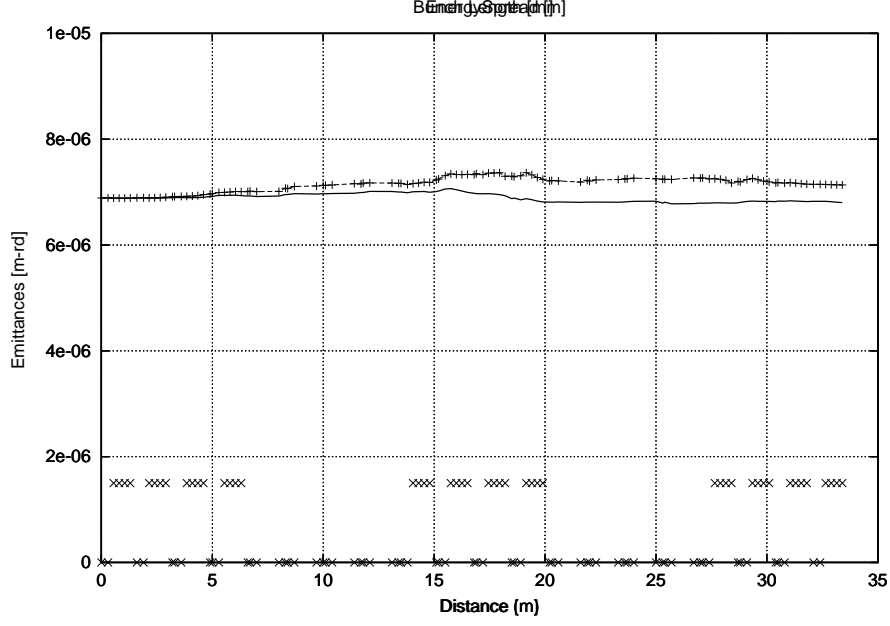


Figure 8: TraFiC4-calculation of emittance growth due to Coherent Synchrotron Radiation effects. Drawn: slice emittance; dotted line: projected emittance. The bending magnets are indicated by the 'x' dots.

the accelerator is

$$\tau = \int_0^L \{1 - \sqrt{[1 + \kappa_0 x(\delta)]^2 + x'(\delta)^2 + y'(\delta)^2}\} dl, \quad (7)$$

where $\kappa_0 = 1/\rho_0$ is the curvature of the design curve and the prime denotes d/dl . For a power expansion $x(\delta) = \delta x_\delta(l) + \delta^2 x_{\delta\delta}(l) + \dots$, and assuming a flat beam line so that $y(\delta) = 0$, the components R_{56} and R_{566} of a bunch compressor are given by

$$\tau = \delta R_{56} + \delta^2 R_{566} + \dots = -\delta \int_0^L \kappa_0 x_\delta dl - \delta^2 \int_0^L [\kappa_0 x_{\delta\delta} + \frac{1}{2} x_\delta'^2 + \frac{1}{2} (\kappa_0 x_\delta)^2] dl. \quad (8)$$

It is therefore important to consider what gives rise to the term $x_{\delta\delta}$.

To express the Lorentz force equation in terms of derivatives with respect to the design path length l rather than t (indicated by a dot), one uses a coordinate system which is co-moving with the reference curve $\vec{R}(l)$ and contains the tangential vector $\vec{t} = \partial_l \vec{R}$. Here a flat reference curve is assumed with a curvature κ_0 which is piece wise 0 or constant. This leads to the representation of a particle's coordinates as

$$\vec{r} = x\vec{e}_x + y\vec{e}_y + \vec{R}, \quad \vec{r}' = x'\vec{e}_x + y'\vec{e}_y + (1 + \kappa_0 x)\vec{t}, \quad (9)$$

$$\vec{r}'' = [x'' - (1 + \kappa_0 x)\kappa_0]\vec{e}_x + y''\vec{e}_y + 2\kappa_0 x'\vec{t}, \quad (10)$$

where $\partial_l \vec{t} = -\kappa_0 \vec{e}_x$ and $\partial_l \vec{e}_x = \kappa_0 \vec{t}$ is used. From $m\gamma\ddot{\vec{r}} = q\dot{\vec{r}} \times \vec{B}$ one obtains the equation of motion by using $v = |\dot{\vec{r}}|$ and

$$\frac{d}{dl} = \frac{|\vec{r}'|}{v} \frac{d}{dt}, \quad \vec{r}' = \frac{|\vec{r}'|}{v} \dot{\vec{r}}, \quad (11)$$

$$\vec{r}'' = \left(\frac{d}{dl} |\vec{r}'| \right) \frac{\dot{\vec{r}}}{v} + \left(\frac{|\vec{r}'|}{v} \right)^2 \ddot{\vec{r}} = \left(\frac{d}{dl} |\vec{r}'| \right) \frac{\vec{r}'}{|\vec{r}'|} + \left(\frac{|\vec{r}'|}{v} \right)^2 \frac{q}{m\gamma} \dot{\vec{r}} \times \vec{B} \quad (12)$$

$$= \left(\frac{\vec{r}'' \cdot \vec{r}'}{|\vec{r}'|^2} \right) \frac{\vec{r}'}{|\vec{r}'|} + |\vec{r}'| \frac{q}{p} \vec{r}' \times \vec{B} \quad (13)$$

$$(14)$$

With $h = 1 + \kappa_0 x$ and $|\vec{r}'|^2 = h^2 + x'^2 + y'^2$, this leads to the equation

$$\frac{1}{|\vec{r}'|^2} \begin{pmatrix} h^2 + y'^2 & -x'y' & -x'h \\ -x'y' & h^2 + x'^2 & -y'h \\ -x'h & -y'h & x'^2 + y'^2 \end{pmatrix} \vec{r}'' = |\vec{r}'| \frac{q}{p} \begin{pmatrix} y'B_l - hB_y \\ hB_x - x'B_l \\ x'B_y - y'B_x \end{pmatrix} \quad (15)$$

The equation of the third row is obsolete, since it can be produced from the first two rows. Taking only the first two rows and assuming the longitudinal field B_l to vanish, leads to

$$\begin{pmatrix} x'' - \kappa_0 h \\ y'' \end{pmatrix} = \frac{1}{h^2} \begin{pmatrix} h^2 + x'^2 & x'y' \\ x'y' & h^2 + y'^2 \end{pmatrix} \left\{ |\vec{r}'| h \frac{q}{p} \begin{pmatrix} -B_y \\ B_x \end{pmatrix} + \frac{h 2\kappa_0 x'}{|\vec{r}'|^2} \begin{pmatrix} x' \\ y' \end{pmatrix} \right\} \quad (16)$$

In order to have the design curve as a reference curve, $(x, x') = 0$ and $(y, y') = 0$ must lead to $x'' = 0$. This leads to the relation $\kappa_0 = \frac{q}{p} B_0$, where B_0 is the vertical field on the reference curve. This finally leads to the two dimensional equation of motion

$$\begin{pmatrix} x'' \\ y'' \end{pmatrix} = \frac{|\vec{r}'|}{h} \frac{q}{p} \begin{pmatrix} h^2 + x'^2 & x'y' \\ x'y' & h^2 + y'^2 \end{pmatrix} \begin{pmatrix} -B_y \\ B_x \end{pmatrix} + \frac{2\kappa_0 x'}{h} \begin{pmatrix} x' \\ y' \end{pmatrix} + h \begin{pmatrix} \kappa_0 \\ 0 \end{pmatrix}. \quad (17)$$

In the complex notation $w = x + iy$ and $B = B_x + iB_y$ this leads to the simplified equation

$$w'' = \frac{\sqrt{w'\bar{w}' + h^2}}{h} \frac{q}{p} [ih^2 B + w'\Im(w'\bar{B})] + \frac{2\kappa_0 \Re(w')}{h} w' + \kappa_0 h. \quad (18)$$

The magnetic field of non-skew dipoles, quadrupoles, and sextupoles is given by

$$\begin{pmatrix} B_x \\ B_y \end{pmatrix} = \frac{p_0}{q} \left[\kappa_0 \begin{pmatrix} 0 \\ 1 \end{pmatrix} + k_q \begin{pmatrix} y \\ x \end{pmatrix} + k_s \begin{pmatrix} xy \\ \frac{1}{2}(x^2 - y^2) \end{pmatrix} \right], \quad B_l = 0. \quad (19)$$

For the computation of the second order dispersion $x_{\delta\delta}$ the y coordinate is set to 0 and one obtains

$$x'' = -\frac{\sqrt{h^2 + x'^2}^3}{h} \frac{p_0}{p} (\kappa_0 + k_q x + k_s \frac{1}{2} x^2) + \frac{2\kappa_0 x'^2}{h} + h\kappa_0. \quad (20)$$

To find the equations of linear motion, one linearizes with respect to x and x' and obtains

$$x^{(1)''} + (k_q + \kappa_0^2) x^{(1)} = 0, \quad (21)$$

with two independent solutions. In order to easily specify a trajectory by its initial conditions $x_i = x(0)$ and $x'_i = x'(0)$, one typically uses the so called cos-like ray x_c and the sin-like ray x_s with

$$x_c(0) = 1, \quad x'_c(0) = 0, \quad x_s(0) = 0, \quad x'_s(0) = 1, \quad x^{(1)} = x_i x_c(l) + x'_i x_s(l). \quad (22)$$

The solution of the nonlinear equation of motion can be found by variation of constants. When the nonlinear equation of motion has the form

$$x^{(n)''} + (k_q + \kappa_0^2)x^{(n)} = f^{(n)}, \quad (23)$$

with a right hand side which depends on small quantities in order n , then variations of constants of the expression $x^{(n)} = A(l)x_c + B(l)x_s$ leads to

$$\begin{pmatrix} x_c & x_s \\ x'_c & x'_s \end{pmatrix} \begin{pmatrix} A' \\ B' \end{pmatrix} = \begin{pmatrix} 0 \\ f^{(n)} \end{pmatrix}. \quad (24)$$

The matrix has a constant determinant since $d/dl(x_c x'_s - x_s x'_c) = x_c x''_s - x_s x''_c = 0$ and it is given by $x_c x'_s - x_s x'_c = 1$. Therefore the inverse of the above matrix is simply obtained by reordering the matrix elements and one obtains

$$\begin{pmatrix} A' \\ B' \end{pmatrix} = f^{(n)} \begin{pmatrix} -x_s \\ x_c \end{pmatrix}, \quad x^{(n)} = x_s \int_0^l f^{(n)} x_c dl - x_c \int_0^l f^{(n)} x_s dl. \quad (25)$$

To find the dispersion x_δ by inserting $x = \delta x_\delta + \dots$, one uses $p = p_0(1 + \delta)$ and linearizes in x and δ ,

$$x_\delta'' + (k_q + \kappa_0^2)x_\delta = \kappa_0. \quad (26)$$

Therefore the dispersion x_δ is given by the well known formula

$$x_\delta = x_s \int_0^l \kappa_0 x_c dl - x_c \int_0^l \kappa_0 x_s dl. \quad (27)$$

Inserting $x = \delta x_\delta + \delta^2 x_{\delta\delta} + \dots$ and taking into account all second orders in δ , one obtains

$$x_{\delta\delta}'' + (k_q + \kappa_0^2)x_{\delta\delta} = f^{(2)}, \quad (28)$$

$$f^{(2)} = -\kappa_0 \left[1 - \frac{1}{2} x_\delta'^2 - \kappa_0 x_\delta (2 - \kappa_0 x_\delta) \right] + k_q x_\delta (1 - 2\kappa_0 x_\delta) - k_s \frac{1}{2} x_\delta^2. \quad (29)$$

The second order dispersion is then given by

$$x_{\delta\delta} = x_s \int f^{(2)} x_c dl - x_c \int f^{(2)} x_s dl. \quad (30)$$

For separated function magnets, where the design curve has no curvature in quadrupoles, the term $k_q \kappa_0$ vanishes. For the bunch compressors which are considered here, the dipole length are around $l_d = 1$ m and their bending angle is between 1° and 5° , therefore $\kappa_0 \in [0.017, 0.087] \frac{1}{\text{m}}$. The slope of x_δ after the first dipole is $x'_\delta \approx l_d \kappa_0$ and

the optic will not allow this slope to become much larger, so that $\frac{1}{2}x'_\delta{}^2 \ll 1$ can be neglected with an error of less than 0.4%. If we consider up to 10 m space between the dipoles, then x_δ will be below 1 m and $\kappa_0 x_\delta \ll 2$ can be neglected with an accuracy of better than 5%. If we also neglect $2\kappa_0 x_\delta$, which is an approximation with an error of less than 20%, one obtains

$$f^{(2)} = -\kappa_0 + k_q x_\delta - k_s \frac{1}{2} x_\delta^2 . \quad (31)$$

In free space and in dipoles, the second order dispersion therefore follows $-x_\delta$. In Quadrupoles, however, $x_{\delta\delta}$ obtains the extra kick $k_q x_\delta$. When $x_{\delta\delta} \approx -x_\delta$, the second order dispersion is focused two times stronger than x_δ . This change of the focusing strength for the second order dispersion with respect to x_δ made it hard to find a bunch compressor which has no second order dispersion at a position where also the first order dispersion vanishes.

Equation (8) can be approximated up to an error of possibly 10% by

$$R_{566} = - \int_0^L \kappa_0 x_{\delta\delta} dl . \quad (32)$$

In the following it will be demonstrated how systems can be constructed for which the ratio R_{566}/R_{56} is zero or slightly positive. The latter would be even better, because it would lead to an acceleration of the beam.

6 FODO Compressor with Matched Dispersion

When a FODO cell has a single pass dispersion $\vec{x}_\delta = (x_\delta, x'_\delta)^T$, the transport matrix \underline{M} for horizontal phase space vectors \vec{x} leads to

$$\underline{M}\vec{x}_i + \delta\vec{x}_\delta = \vec{x}_f . \quad (33)$$

Since the first order periodic dispersion $\vec{\eta}_\delta$ satisfies $\underline{M}\vec{\eta}_\delta + \vec{x}_\delta = \vec{\eta}_\delta$, it can be computed by

$$\vec{\eta}_\delta = (\underline{1} - \underline{M})^{-1} \vec{x}_\delta . \quad (34)$$

Once $\vec{\eta}_\delta$ is known, the term $k_q \eta_\delta$ can be computed, which then in turn leads to the second order single pass dispersion $\vec{x}_{\delta\delta}$ and finally to the second order periodic dispersion $\vec{\eta}_{\delta\delta}$.

For simple thin lens FODO cells with focal strength $\pm k$ for the two families of quadrupoles, with bend angles b , and with a length which leads to a phase advance ϕ_x and $s = \sin(\frac{\phi_x}{2})$, one can compute the first and second order periodic dispersion at the focusing and the defocusing quadrupole as

$$\vec{\eta}_\delta^{max} = \begin{pmatrix} \frac{b}{k}(\frac{1}{s} + \frac{1}{2}) \\ 0 \end{pmatrix} , \quad \vec{\eta}_\delta^{min} = \begin{pmatrix} \frac{b}{k}(\frac{1}{s} - \frac{1}{2}) \\ 0 \end{pmatrix} , \quad \vec{\eta}_{\delta\delta}^{max} = \vec{\eta}_{\delta\delta}^{min} = \begin{pmatrix} \frac{b}{k} \frac{1}{s} \\ 0 \end{pmatrix} . \quad (35)$$

With $R_{56} = -\int_0^L \kappa_0 x_\delta dl$ and with the approximation $R_{566} = -\int_0^L \kappa_0 \eta_{\delta\delta} dl$ this leads to the time of flight terms

$$R_{56} = -\frac{b^2}{4k_s}[7 + \cos(\phi_x)] , \quad R_{566} = -\frac{b^2}{4k_s}[9 - \cos(\phi_x)] . \quad (36)$$

The ratio $r = R_{566}/R_{56} \approx 1$ lead us to try to base a bunch compressor on a FODO lattice with periodic dispersion. Coming from a linear accelerator into the bunch compressor FODO cells, the dispersion will not be the periodic dispersion but after the first FODO cell it will be the single pass dispersion \vec{x}_δ^1 . After n cells, the dispersion would be

$$\vec{x}_\delta = \underline{M}^{n-1} \vec{x}_\delta^1 + \underline{M}^{n-2} \vec{x}_\delta^1 + \dots + \vec{x}_\delta^1 = (\underline{1} - \underline{M}^n)(\underline{1} - \underline{M})^{-1} \vec{x}_\delta^1 = (\underline{1} - \underline{M}^n) \vec{\eta}_\delta . \quad (37)$$

The correctness of the second equivalence is checked by applying $(\underline{1} - \underline{M})$ from the right hand side. Whenever $\underline{M}^n = -\underline{1}$, which corresponds to a betatron phase advance of π , \vec{x}_δ is $2\vec{\eta}_\delta$. When rectangular bends are used in a FODO, then the transport matrix does not depend on the bending angle. The dispersion \vec{x}_δ^1 in equation (27) is however linearly related to the bending angle. If therefore n FODO cells are build with half the bending angles, then \vec{x}_δ after these cells will be $(\underline{1} - \underline{M}^n)(\underline{1} - \underline{M})^{-1} \vec{x}_\delta^1 \frac{1}{2}$ and for a phase advance of π this is equivalent to the periodic dispersion $\vec{\eta}_\delta$. This constitutes a short prove of the well known half strength dispersion matching described in [7, 8]. FODO cells with reversed bend direction have $-\eta_\delta$ as their periodic dispersion. If the FODO cells and the cells with reduced bending strength should bend in opposite direction, then the latter would need to have a dispersion of $-\eta_\delta$. But this can not be achieved for any number n of cells.

In passing we note that it was also tried to use the missing magnet scheme for creating the periodic dispersion, but this was less advantageous for the second order dispersion. For this scheme n FODO cells are followed by m FODO cells without bending magnets. The total dispersion after this scheme will be

$$\vec{x}_\delta = \underline{M}^m (\underline{1} - \underline{M}^n)(\underline{1} - \underline{M})^{-1} \vec{x}_\delta^1 . \quad (38)$$

This is the periodic dispersion $\vec{\eta}_\delta$ whenever $\underline{1} - \underline{M}^n = \underline{M}^{-m}$. When the transport matrix is expressed in the normal form space of the FODO, it describes simply a rotation by the phase advance ϕ_x and leads to

$$\begin{pmatrix} 1 - \cos(n\phi_x) & -\sin(n\phi_x) \\ \sin(n\phi_x) & 1 - \cos(n\phi_x) \end{pmatrix} = \begin{pmatrix} \cos(m\phi_x) & -\sin(m\phi_x) \\ \sin(m\phi_x) & \cos(m\phi_x) \end{pmatrix} . \quad (39)$$

The off diagonal condition implies either $m\phi_x = -n\phi_x + \pi \bmod 2\pi$, which is incompatible with the diagonal equations, or $m\phi_x = n\phi_x \bmod 2\pi$, which together with the equations on the diagonal leads to $m\phi_x = \pm\pi/3 \bmod 2\pi$.

This scheme could be used to match to the negative dispersion, since $(\underline{1} - \underline{M}^n)$ can be $-\underline{M}^{-m}$, which is the case when

$$\begin{pmatrix} 1 - \cos(n\phi_x) & -\sin(n\phi_x) \\ \sin(n\phi_x) & 1 - \cos(n\phi_x) \end{pmatrix} = \begin{pmatrix} -\cos(m\phi_x) & \sin(m\phi_x) \\ -\sin(m\phi_x) & -\cos(m\phi_x) \end{pmatrix} . \quad (40)$$

This requires either $m\phi_x = -n\phi_x \bmod 2\pi$ or $m\phi_x = n\phi_x + \pi \bmod 2\pi$. The first equation is incompatible with the diagonal equations. The second leads to $n\phi_x = \pm\pi/3 \bmod 2\pi$. This option however turned out to be not useful, since it requires at least 4 FODO cells for the dispersion match.

The FODO compressor which performed best uses the half bend matching scheme of two FODOs with $\phi_x = 90^\circ$. The optics is shown in figure 9. The first order dispersion

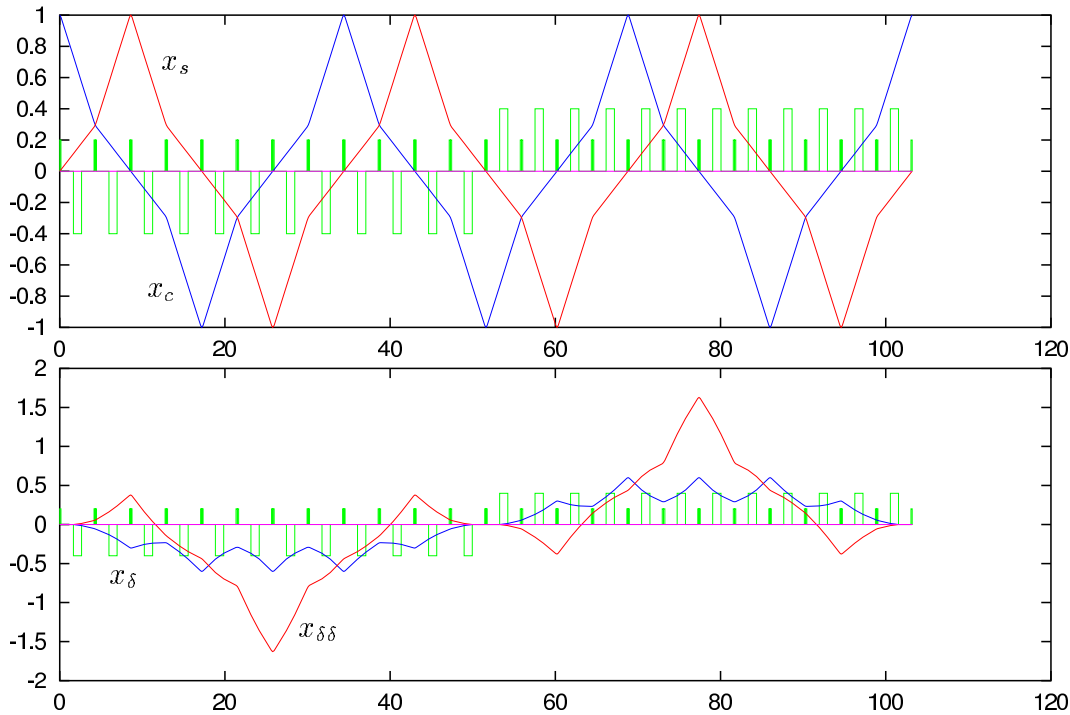


Figure 9: Top: The cos-like (x_c) and the sin-like (x_s) ray. Bottom: the first and second order dispersion in the FODO compressor with matched dispersion.

is periodic in 4 of the 12 FODO cells. At a focusing quadrupole where the second order dispersion has a maximum, a weak sextupole was inserted to make $x'_{\delta\delta} = 0$ and a mirror symmetric system was used to bring the second order dispersion back to zero. In order to make the total beam direction parallel, the system of 6 FODO cells was repeated in a mirror symmetric way.

This FODO bunch compressor has a ratio $R_{566}/R_{56} = 2.4$ which avoids the longitudinal emittance increase observed with the previously mentioned FODO compressor. Additionally the beam is accelerated by about 500MeV. The resulting longitudinal phase space for 12 ellipses around emittances between 0σ and 3σ after the bunch compressor are shown in figure 11. The slight deformation at high amplitudes would be tolerable.

However, it turns out that, even after $\vec{x}_{\delta\delta}$ is eliminated, the higher order dispersions lead to a non-negligible increase of the emittance. The higher order dispersions up to order 15 were computed with COSY INFINITY [9] and are given bellow. It is

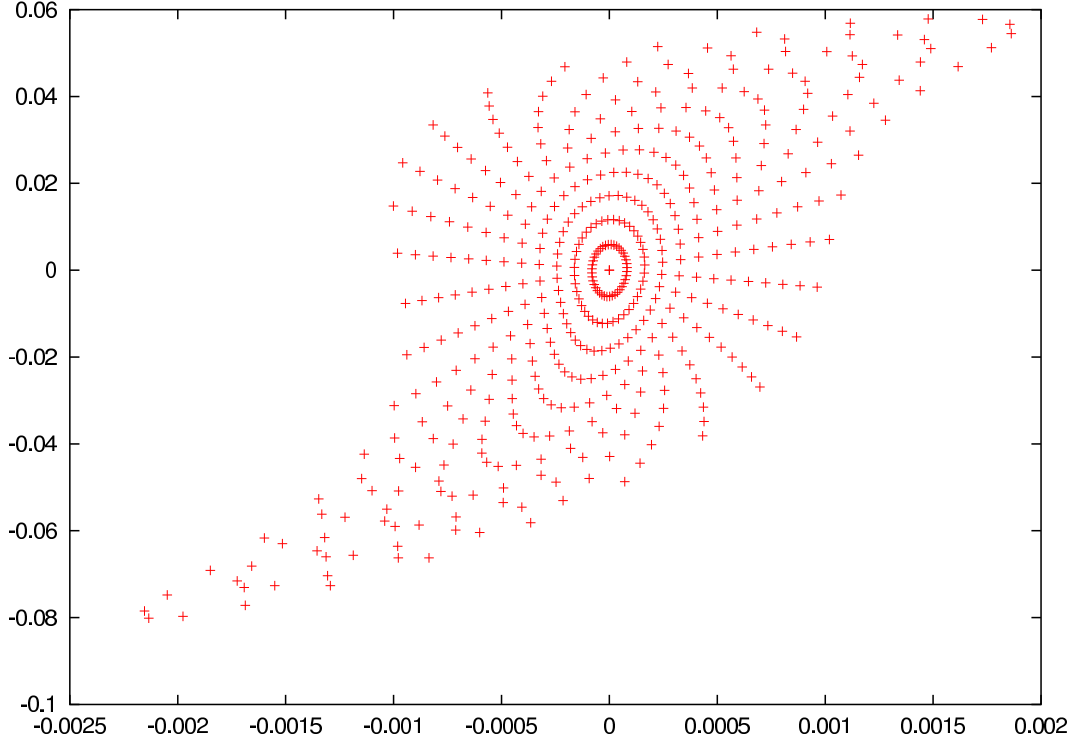


Figure 10: Twelve ellipses around longitudinal emittances of up to 3σ after being tracked through the FODO bunch compressor with matched dispersion. Here the 7th order dispersion was corrected, but the longitudinal phase space is not influenced significantly by the higher order dispersion correction.

normalized to a 3σ energy deviation of 10% with $\delta_{3\sigma} = \delta/0.1$,

$$\begin{aligned}
 x(\delta)/\text{mm} = & -19\delta_{3\sigma}^3 + 4.2\delta_{3\sigma}^4 + 16\delta_{3\sigma}^5 - 8.9\delta_{3\sigma}^6 - 1.2\delta_{3\sigma}^7 \\
 & + 2.7\delta_{3\sigma}^8 - 1.1\delta_{3\sigma}^9 + 0.1\delta_{3\sigma}^{10} + 0.09\delta_{3\sigma}^{11} - 0.06\delta_{3\sigma}^{12} \\
 & + 0.02\delta_{3\sigma}^{13} - 0.005\delta_{3\sigma}^{14} + 0.0004\delta_{3\sigma}^{15} .
 \end{aligned} \tag{41}$$

After multipoles are inserted inside the 3rd and 9th quadrupole to correct the dispersion up to order 7, the first 15 orders of the dispersion are given by

$$\begin{aligned}
 x(\delta)/\text{mm} = & 7.6\delta_{3\sigma}^8 + 10\delta_{3\sigma}^9 - 3.0\delta_{3\sigma}^{10} - 5.1\delta_{3\sigma}^{11} + 0.9\delta_{3\sigma}^{12} \\
 & + 0.8\delta_{3\sigma}^{13} - 0.1\delta_{3\sigma}^{14} - 0.1\delta_{3\sigma}^{15} .
 \end{aligned} \tag{42}$$

The remaining horizontal emittance blowup after the correction of the 7th order dispersion is shown in figure 11 (left). The ellipse around the 1σ transverse emittance has been transported through the illustrated FODO bunch compressor for particles with up to 2σ energy deviation. This figure shows that other nonlinear aberrations are not critical and that the correction of the 7th order dispersion is sufficient. Correcting only up to order 6 was however not sufficient. In figure 11 (right) energy deviations of up to 2σ have been assumed for particles on the 1σ ellipse. This shows that the higher order

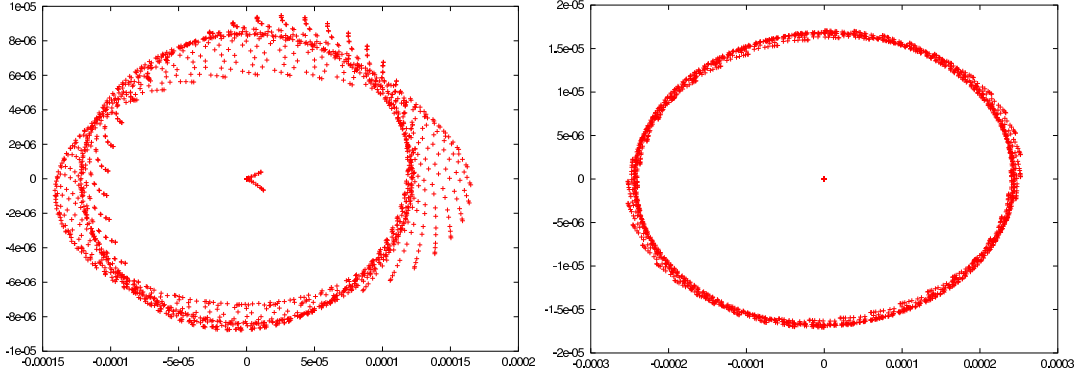


Figure 11: Left: The ellipse around the horizontal 1σ emittance for energy deviations of up to 2σ after being tracked through the FODO compressor after the 7th order dispersion is corrected. Right: The ellipse around the horizontal 2σ emittance for energy deviations of up to 1σ after being tracked through this FODO compressor.

dispersion prohibits the use of a FODO bunch compressor for the large energy spread of up to 10% at 3σ of the energy distribution. For smaller energy spreads, FODO compressors of this type might be feasible.

7 360° Compressor

Every quadrupole at a dispersive section contributes to the higher order dispersion due to the kick $xk_q \frac{2\theta}{p}$ in equation (20). The higher order dispersions might therefore be reduced by reducing the horizontal phase advance from $3 \cdot 360^\circ$ in the FODO compressor to a smaller value. While the ratio between R_{566} and R_{56} is small and positive in the discussed FODO compressor even without the aid of sextupoles, no such solution was found for a device with significantly smaller phase advance. However, sextupoles can be used to manipulate the integral $R_{566} \approx -\int_0^L \kappa_0 x_{\delta\delta} dl$. This has to be done while guaranteeing $\vec{x}_{\delta\delta} = 0$. In addition, such sextupoles introduce higher order aberrations, which should be kept small. To meet these requirements, a symmetric arrangement was sought where $x_{\delta\delta} = 0$ and $x'_{\delta\delta} = 0$ are guaranteed by two mirror symmetric sections in the device. Additionally the geometric aberrations introduced by the sextupoles can be canceled by a phase advance of 180° between sextupoles [10, 11].

As shown in figure 12 the two requirements: (a) of having two symmetry planes and (b) of having each sextupole compensated by a second equivalent sextupole which is 180° apart in betatron phase, can only be satisfied when the total betatron phase advance is at least 360° . A suitable optic without sextupoles is shown in figure 13. At the first symmetry plane the dispersion is zero, but its slope x'_δ is not zero. An anti-symmetric arrangement of the dipole magnets leads to $\vec{x}_\delta = 0$ at the central symmetry plane. Furthermore x_s and x_c have symmetry properties with respect to the first and to the central symmetry plane. The product $k_q x_\delta$ and the curvature κ_0 are antisymmetric

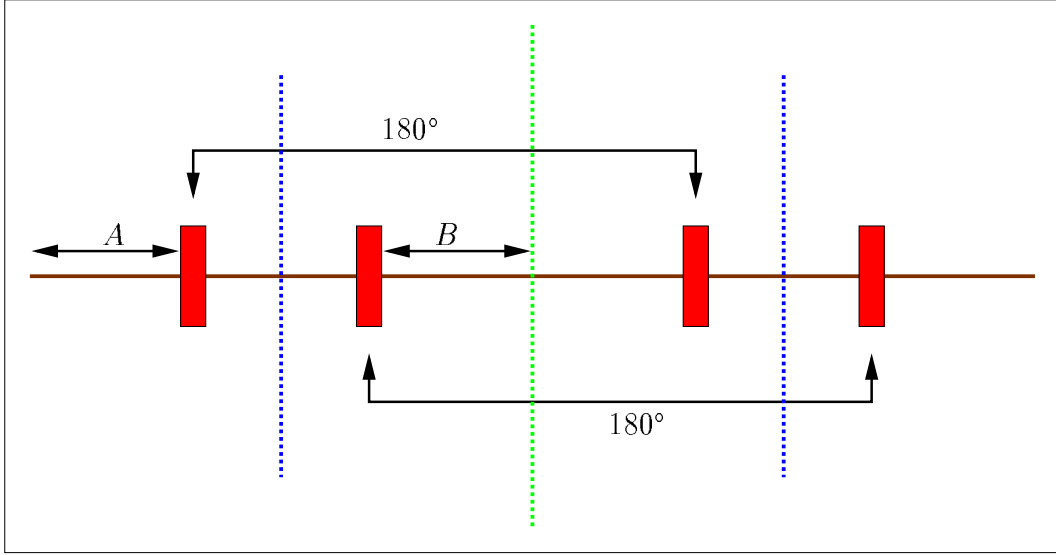


Figure 12: The symmetry plan (green central vertical line) requires that every inserted sextupole (red boxes) has to be accompanied by a second sextupole. The condition of having sextupoles in pairs with a phase of 180° in between leads to two more sextupoles. The requirement of a second symmetry plane (two red vertical lines) leads to $A = B$ and therefore to a total phase advance of 360° .

with respect to the first plane, and therefore the second order dispersion

$$x_{\delta\delta} = x_s \int_0^L x_c(-\kappa_0 + k_q x_\delta) dl - x_c \int_0^L x_s(-\kappa_0 + k_q x_\delta) dl = x_s \int_0^L x_c(-\kappa_0 + k_q x_\delta) dl . \quad (43)$$

Since $x_s = 0$ in the central plane, also $x_{\delta\delta} = 0$. The slope $x'_{\delta\delta}$ is not zero, since $x'_s = -1$ in the central plane.

An antisymmetric arrangement of the bending angles with respect to the central plane then eliminates $\vec{x}_{\delta\delta}$ in the final plane. In order not to destroy this property, sextupoles, if applied, need to have the same symmetry as the dipole fields. The following list illustrates the symmetry properties:

Symmetry at		1. plane	central plane
(a)	κ_0	-	-
(b)	k_q	+	+
(c)	k_s	-	-
(d)	x_c	-	+
(e)	x_s	+	-
(f)	x_δ	-	-
(g)	$x_{\delta\delta}$	none	-

This arrangement has a ratio $R_{566}/R_{56} = -2.8$ and sextupoles have to be used to bring the large excursions of $x_{\delta\delta}$ to the other side of the design curve. The sextupole kicks

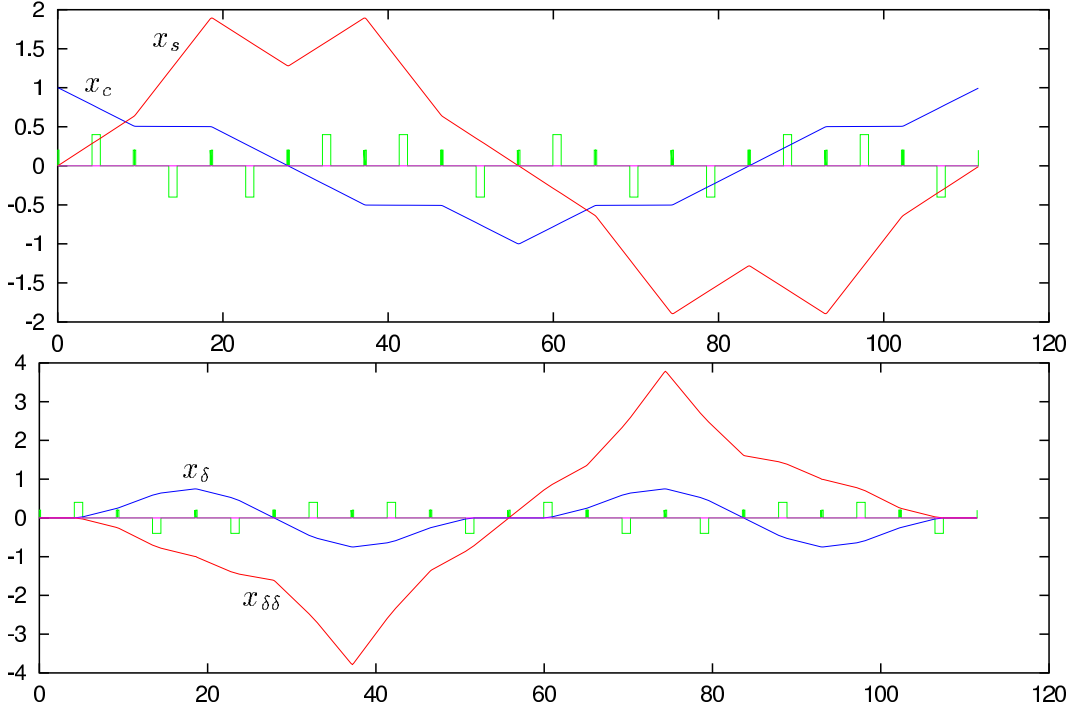


Figure 13: Top: The cos-like (x_c) and the sin-like (x_s) ray. Bottom: the first and second order dispersion in the 360° compressor with matched dispersion.

$\frac{1}{2}k_s x_\delta^2$ are effective when the dispersion is large, and therefore the first sextupole was placed after the third quadrupole. The antisymmetric requirements lead to three more sextupoles, one with reversed sign before the fifth quadrupole and two more sextupoles, each shifted by 180° with respect to the first two sextupoles. The requirement of canceling geometric second order aberrations by this 180° phase advance is only possible with either two symmetric or with two antisymmetric planes. With mixed symmetries, the sextupoles would also be π apart but they would need to have opposite signs which would not lead to cancelation but to a buildup of aberrations.

For aberrations we use the notation

$$x_f = x_i x_c + x'_i x_s + \delta x_\delta + x_i^2 x_{xx} + x_i x'_i x_{xx'} + x_i'^2 x_{x'x'} + \dots \quad (44)$$

$$x'_f = x_i x'_c + x'_i x'_s + \delta x'_\delta + x_i^2 x'_{xx} + x_i x'_i x'_{xx'} + x_i'^2 x'_{x'x'} + \dots \quad (45)$$

$$(46)$$

The following list shows that nearly all second order aberrations due to the sextupoles are compensated by this setup,

Aberration	Integral form	
		0 due to symmetry in above table
x_{xx}	$\frac{1}{2} \int_0^L k_s x_s x_c^2 dl$	0 due to (c1), (d1), and (e1)
$x_{xx'}$	$\int_0^L k_s x_s^2 x_c dl$	0 due to (c2), (d2), and (e2)
$x_{x'x'}$	$\frac{1}{2} \int_0^L k_s x_s^3 dl$	0 due to (c1) and (e1)
x'_{xx}	$-\frac{1}{2} \int_0^L k_s x_c^3 dl$	0 due to (c2) and (d2)
$x'_{xx'}$	$-\int_0^L k_s x_s x_c^2 dl$	0 due to (c1), (d1), and (e1)
$x'_{x'x'}$	$-\frac{1}{2} \int_0^L k_s x_s^2 x_c dl$	0 due to (c2), (d2), and (e2)
$x_{\delta\delta}$	$\frac{1}{2} \int_0^L k_s x_s x_\delta^2 dl$	0 due to (c1), (e1), and (f1)
$x'_{\delta\delta}$	$-\frac{1}{2} \int_0^L k_s x_c x_\delta^2 dl$	0 due to (c2), (d2), and (f2)
$x_{x\delta}$	$\int_0^L k_s x_s x_c x_\delta dl$	0 due to (c1/2), (d1/2), (e1/2), and (f1/2)
$x'_{x'\delta}$	$-\int_0^L k_s x_s x_c x_\delta dl$	0 due to (c1/2), (d1/2), (e1/2), and (f1/2)

The only second order aberrations which are not canceled are

$$x_{x'\delta} = \int_0^L k_s x_s^2 x_\delta dl , \quad x'_{x\delta} = - \int_0^L k_s x_c^2 x_\delta dl . \quad (47)$$

These aberrations cannot be compensated by an antisymmetry, since x_s^2 and x_c^2 are symmetric with respect to any symmetry plane, and also $k_s x_\delta$ is symmetric. But these aberrations would be avoided if the sextupoles were chosen in a symmetric rather than in an antisymmetric way. The following two cases can be distinguished:

(a) k_s is chosen symmetric at both symmetry planes. All second order geometric aberrations would still cancel due to the phase advance of 180° between equal sextupoles. Also the second order dispersion would still vanish at the end since the integrals in the above table would still cancel due to the antisymmetry properties of x_s and x_c . However, while $k_s x_\delta$ is antisymmetric and the integrals in equation (47) both vanish, the aberrations $x_{x'\delta}$ and $x'_{x\delta}$ would not cancel.

But the terminal disadvantage of this strategy is the fact that R_{566} cannot be altered in this way. In fact, R_{566} of an arrangement with symmetry plane and $\vec{x}_\delta = 0$ at its end is not influenced by an arrangement of sextupoles for which $x_\delta k_s$ is antisymmetric and for which the fundamental rays x_s and x_c are symmetric or antisymmetric. We denote the symmetric ray by x_+ and the antisymmetric one by x_- . The contribution of the sextupoles to $x_{\delta\delta}$ is then given by

$$\begin{aligned} & \pm (x_+ \int_0^l x_- k_s x_\delta^2 dl - x_- \int_0^l x_+ k_s x_\delta^2 dl) \\ &= x_+ S(l) + x_- (K + A(l)) \text{ or } x_- S(l) + x_+ (K + A(l)) , \end{aligned} \quad (48)$$

The first possibility follows for a symmetric arrangements of k_s and the second for an antisymmetric arrangement. Here $S(l)$ is some symmetric and $A(l)$ some antisymmetric function of l with respect to the symmetry plane; K is a constant. This follows from the fact that the integral over an antisymmetric function is a symmetric function and the integral over a symmetric function is a constant plus an antisymmetric function. The contribution of the sextupoles to R_{566} is given by

$$\pm R_{566}^{k_s} = - \int_0^L (\kappa_0 x_\pm S(l) + \kappa_0 x_\mp (K + A(l))) dl , \quad (49)$$

where the upper sign corresponds to symmetric sextupole arrangements. Since $\vec{x}_\delta = 0$ at the end of the device, the curvature κ_0 in the dipoles has the same symmetry as x_δ . Since $k_s x_\delta$ is antisymmetric, $\kappa_0 x_\pm S(l)$ is antisymmetric since for the upper sign k_s is symmetric and κ_0 antisymmetric and for the lower sign vice versa. Two parts of the integral therefore have an antisymmetric integrand and vanish, leaving

$$R_{566}^{ks} = -K \int_0^L \kappa_0 x_\mp dl . \quad (50)$$

According to equation (27) is proportional to either x_δ or x'_δ after the bunch compressor, which are both zero. This proves that in the given 360° compressor a symmetric arrangement of sextupoles, while not crating the aberration $x_{x'\delta}$ and $x'_{x\delta}$ cannot be used to influence R_{566} .

(b) When the sextupoles are symmetric with respect to only one of the symmetry planes, but antisymmetric with respect to the other, then all four chromatic aberrations $x_{x'\delta}$, $x'_{x\delta}$, $x_{x\delta}$, and $x'_{x'\delta}$ would not be created by the sextupoles. But some geometric second order aberrations would be created. However, in the given arrangement this might not be very significant since all problems are related to the very large energy spread of the beam. But again R_{566} could not be manipulated and either $x_{\delta\delta}$ or $x'_{\delta\delta}$ would become non-zero due to the sextupoles.

The only possibility to adjust R_{566} is therefore the applied antisymmetric arrangements of sextupoles with respect to both symmetry planes. The critical aberrations of such a 360° compressor are therefore the energy dependent focusing errors and the higher order dispersions.

The 15th order power expansion of the dispersion relative to an energy spread $\delta = 0.1 \cdot \delta_{3\sigma}$ with a 3σ value of 10%, which corresponds roughly to the desired value of the bunch compressor, at the end of the system is

$$\begin{aligned} x(\delta)/\text{mm} = & -140\delta_{3\sigma}^3 + 50\delta_{3\sigma}^4 + 46\delta_{3\sigma}^5 + 71\delta_{3\sigma}^6 + 97\delta_{3\sigma}^7 \\ & + 83\delta_{3\sigma}^8 + 15\delta_{3\sigma}^9 + 17\delta_{3\sigma}^{10} - 32\delta_{3\sigma}^{11} - 0.7\delta_{3\sigma}^{12} \\ & + 6.2\delta_{3\sigma}^{13} - 1.2\delta_{3\sigma}^{14} + 1.4\delta_{3\sigma}^{15} . \end{aligned} \quad (51)$$

In this 360° bunch compressor even correcting $\vec{x}_{\delta\delta}$ up to order 7 is not sufficient. The dispersion coefficients up to order 15 are then given by

$$\begin{aligned} x(\delta)/\text{mm} = & 5195\delta_{3\sigma}^8 + 8010\delta_{3\sigma}^9 - 9657\delta_{3\sigma}^{10} - 1856\delta_{3\sigma}^{11} \\ & + 1206\delta_{3\sigma}^{12} + 8362\delta_{3\sigma}^{13} - 16401\delta_{3\sigma}^{14} - 696652\delta_{3\sigma}^{15} . \end{aligned} \quad (52)$$

Figure 14 (left) shows the horizontal 1σ ellipse for particles with up to 2σ energy spread after passing the bunch compressor. Obviously the dispersion is still far too large. Figure 14 (right) shows the horizontal 2σ ellipse for particles with up to 1σ energy deviation. The dispersion effect has disappeared completely, due too its high order dependence on δ , but the energy dependent optics becomes dominant.

Figure 15 shows the longitudinal phase space of up to 3σ after having been tracked through the 360° bunch compressor. Since R_{566} has been matched to 0, the longitudinal

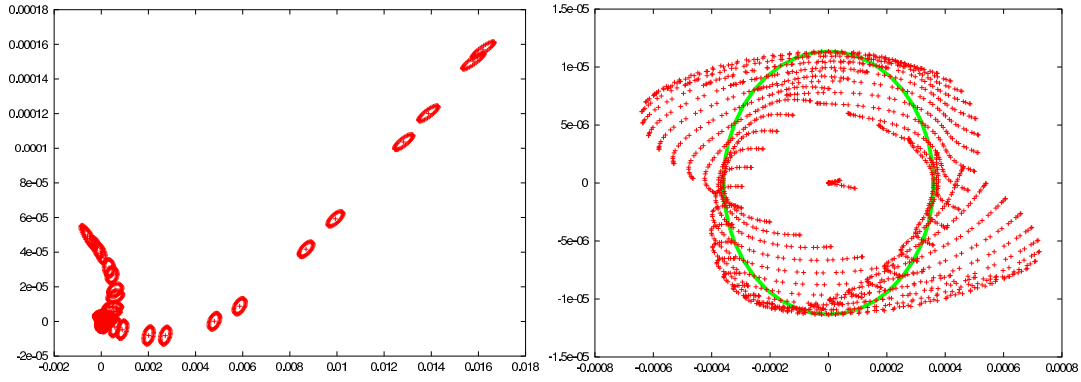


Figure 14: Left: The ellipse around the horizontal 1σ emittance for energy deviations of up to 2σ after being tracked through the FODO compressor after the 7th order dispersion is corrected. Right: The ellipse around the horizontal 2σ emittance for energy deviations of up to 1σ after being tracked through this FODO compressor. The ellipse corresponds to on energy particles ($\delta = 0$).

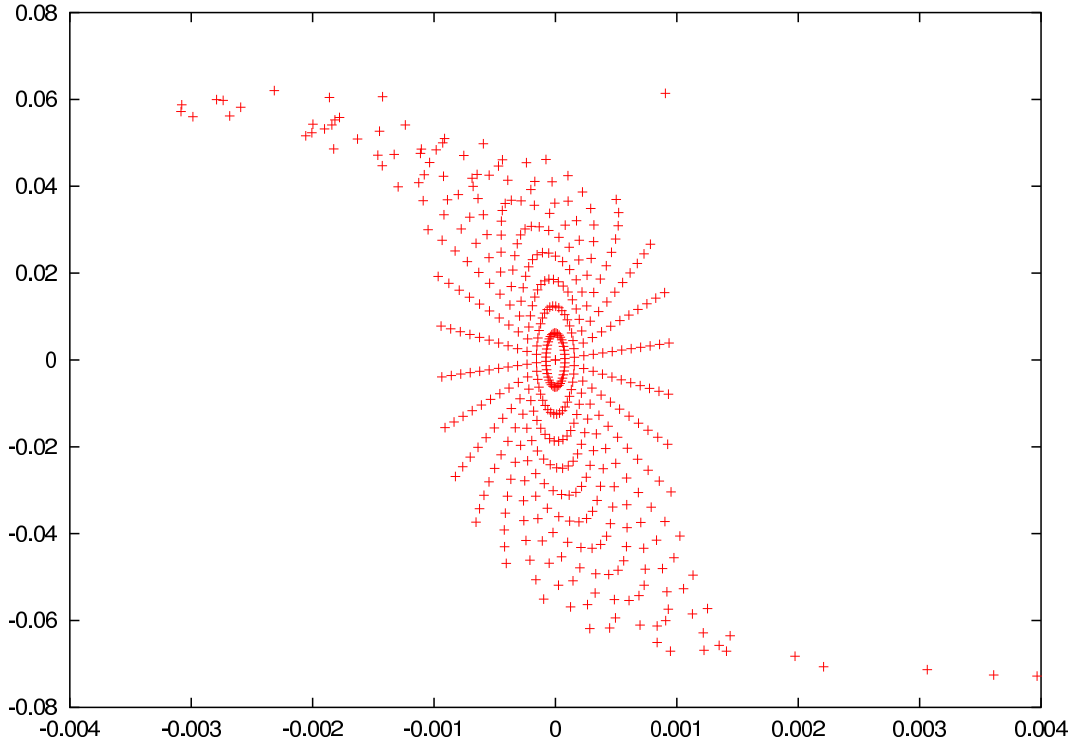


Figure 15: Twelve ellipses around longitudinal emittances of up to 3σ after being tracked through the FODO bunch compressor with matched dispersion.

dynamics is satisfactory. The longitudinal phase space motion is sufficiently linear due to $R_{566} = 0$. But also here higher order effects can be observed.

For the here described application with a 3σ energy spread of 10% this bunch

compressor is not suitable. For applications with less energy spread it might be feasible however.

8 Required Accuracy for a Wiggler Compressor

Except for the wiggler compressor described in this paper, all other arrangements which have been analyzed have large higher order dispersion coefficients. This could indicate that the symmetric magnetic fields of the wiggler compressor, which leads to a cancelation of all higher order terms, are very sensitive to misalignments. The cancelation would be mostly violated if there was an edge focusing at one of the parallel faced magnets. The power expansion of the dispersion after such a system which has a pole face angle of 0.5 mrad at the exit of the second magnet is given by

$$\begin{aligned}
 x(\delta)/\text{mm} = & 0.028\delta_{3\sigma} - 0.0087\delta_{3\sigma}^2 - 0.0022\delta_{3\sigma}^3 + 0.0018\delta_{3\sigma}^4 \\
 & - 0.00065\delta_{3\sigma}^5 + 0.00017\delta_{3\sigma}^6 - 0.000037\delta_{3\sigma}^7 .
 \end{aligned}
 \tag{53}$$

The edges of the parallel faced magnets of the wiggler bunch compressor therefore has to be parallel up to less than half a m rad. This accuracy of 0.1 mm over a 50 cm magnet pole face should be achievable.

References

- [1] R. Brinkmann, G. Materlik, J. Roßbach, A. Wagner (editors), Conceptual Design of a 500 GeV e+e- Linear Collider with Integrated X-ray Laser Facility, *Report DESY-97-048* and *Reprot ECFA-97-182* (1997)
- [2] R. Brinkmann, Basic Assumptions for the TESLA TDR, *DESY internal note* (2000)
- [3] P. Emma, Bunch Compressor Beamlines for the TESLA and S-Band Linear Colliders, *Report TESLA-95-17* (1995)
- [4] P. Emma, Bunch Compressor Options for the New TESLA Parameters, *Report TESLA-98-31* (1998)
- [5] H. Grote, F. Iselin, The MAD Program, *Report CERN/SL/90-13(AP)* (1996)
- [6] M. Dohlus, A. Kabel, T. Limberg *NIMA***445**, pp. 338-342 (2000)
- [7] F. Willeke, Verbotene Q Werte bei PETRA, *Report DESY PET-81/28* (1981)
- [8] K. Steffen, Periodic Dispersion Suppressors, *Report DESY HERA-81/19* (1981)
- [9] M. Berz, K. Makino, K. Shamseddine, G. H. Hoffstaetter, and W. Wan, COSY INFINITY and its applications in nonlinear dynamics, in *Computational Differentiation, Techniques, Applications, and Tools*, pp. 363-367, SIAM (1996)

- [10] K. L. Brown, A Second-Order Magnetic Optical Achromat, *Report SLAC-PUB-2257* (February 1979)
- [11] K. L. Brown and R. V. Servranckx, First- and Second-Order Charged Particle Optics, *Report SLAC-PUB-3381* (1984)